Conference on Architectural and Structural Applications of Glass
Ghent University, June 2020.

Challenging Glass 7

Experimental and numerical assessment of permeability functions in Closed Cavity Facades

Guido Lori [a], Kjartan Van Den Brande [b], Nathan Van Den Bossche [b], Henk De Bleecker [c], Jan Belis [b]
[a] *PermasteelisaGroup, Italy, g.lori@permasteelisagroup.com*
[b] *Ghent University, Belgium*
[c] *PermasteelisaGroup, The Netherlands*

This paper is the second in a series on the behavior of closed cavity facades (CCF) under termo-mechanical loading excitations. CCF are a novel trend for sustainable high quality double skin façade solutions, characterized by a minimal maintenance demand. The air cavity is designed according to stringent air tightness requirements, provided with a small dry air flow that preserves the relative humidity, minimizing the risk for condensation and dust ingress. This extremely reduced permeability, with respect to typical double skin design, gives a scenario in conflict with the general prescriptions for the structural calculations of double skins under wind and climatic loading. This paper is the second of a series of three documents that aim to identify the structural shortcomings in the current codes and to propose efficient calculation methods and modifications to the current calculation strategies in order to overcome a critical design paradox in double skin and in particular CCF aim to reach the highest sustainability performance, by means of outstanding thermal and acoustic insulation efficiency and providing the cavity with a clean and dry environment, suitable for a significant upgrade of the façade life expectancy. On the other hand, an overly conservative calculation approach is generally against the optimization of the sustainability performance indices, determining an excessive use of materials and then impacting the overall life cycle cost under several perspectives. In particular, the objective of this second paper is to describe in a measurable way the permeability behaviour of a CCF, defining statistical variability and nonlinearity effects measured during dedicated experimental testing. The permeability functions represent a fundamental input for the proposed assessment tool introduced by the first paper and it will be seen that an accurate quality control during the manufacturing can ensure the robustness of an optimized calculation approach, based on the load sharing mechanism between the skins. In the third paper it will be shown that the proposed tool, fed by the experimental permeability functions, renders adequate to predict the façade structural behaviour under the superimposition of thermal loading, wind loading and dry air flow effects, when compared with measurements collected during outdoor testing on a façade specimen.

Keywords: Double Skin, Climatic Loads, Wind Loads, Load Sharing

1.Introduction

Double skin facades are always source of uncertainties regarding their mechanical behavior under wind loading, when researchers look for a compromise between safety and the possibility to apply a reduction of the net pressure coefficients. If the load sharing mechanism for fully impermeable cavities (insulating glazing units) is a well described and understood phenomenon, on the contrary the wide range of applications for permeable double skins would require an extensive investigation through completely different scenarios in order to characterize the impact of local and global effects on the net pressure build up. Standards and best practices define simplified and comprehensive analytical approaches and aim to present to the designer a way for an optimized yet safe design approach, but in case of double skin facades there is a lack of guidelines in this sense. The current Eurocode revision for wind loading, EN1991-1-4, is only proposing a discount for the pressure coefficient on the permeable skin, when it is possible to classify one of the skins as permeable and the other impermeable. The classification is carried out by means of the impermeability limit, defined as 0.1% of the skin surface for the equivalent opening area of the skin. Under these circumstances, the designer is allowed to reduce by one third the net pressure coefficient in case of pressure and by two third in case of suction. Although it is not fully clear whether the guideline applies regardless of construction type of the double skin, for instance compact unitized system or large open cavity with an external skin in front of the air barrier single skin, it is evident that the guideline looks at the typical ventilated double skin scheme. In this case the analogy with the classical pressure equalization scheme for the rainscreen is quite robust: generally, the outer skin is the rainscreen barrier and provided with a certain opening surface A_{RS}, while the inner skin is the air barrier skin and it is characterized by A_{AB} openings. Rainscreeen strategy states that A_{RS} should be at least ten times bigger than A_{AB} in order to provide the cavity with pressure equalization to the external environment. EN1991-1-4 statements for permeable skins is based on the evidence that a rate of pressure equalization about 99% is reached if the above quick design guideline is adopted for the ratio of the openings. However, when both the skins are impermeable the code supports only the discount of the internal pressure part for the less stiff skin, which basically neglects any load sharing effect. The contradiction is quite evident, as in a comprehensive and organic approach, the code should merge in the same theory the scenario of fully closed (insulating units) and fully pressure equalized (ventilated double skins) as the two extreme scenarios.

Although in the past the impermeable/impermeable case was not of applicative importance, during recent years a novel type of façade has been developed which has permeability conditions close to the scenario of a double air barrier. The design principle in terms of watertightness strategy is different than ventilated facades, as there is no intent to equalize the cavity to one of the two boundaries, but just to make both the skins as much airtight as possible and control the cavity permeability by intended ventilation holes provided through the framing members. Micro-ventilation is provided by the balance between a low dry air flow continuously pumped into the cavity and the air flow exchange through the intended holes. This different façade concept has been understandably called Closed Cavity Façade (CCF) and Fig. 1 shows at the left side one typical design for one commercial technology of this façade type, named mfree-S$^{CCF.}$

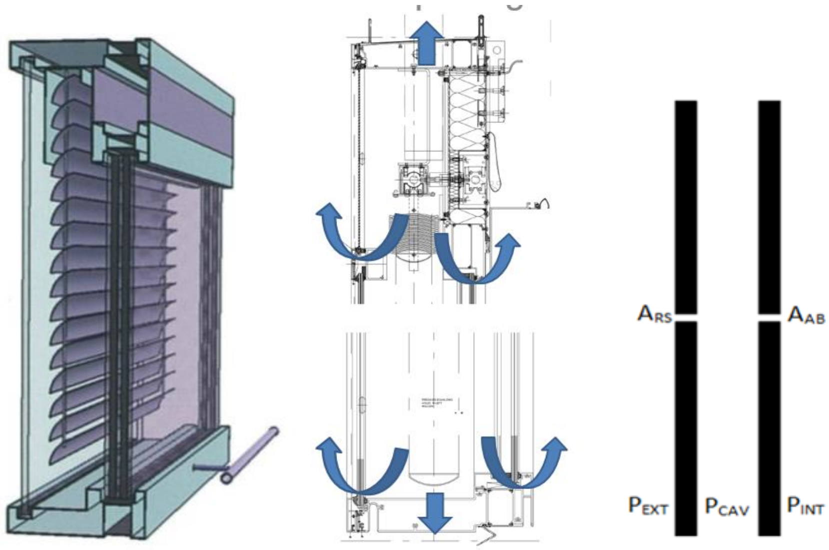

Fig. 1 Typical mfree-S^{CCF} design (left) with permeability sources (mid) and equivalent rainscreen scheme (right)

Differently from the classical rainscreen scheme, for which the surface openings have a clear predominance of A_{RS} with respect to A_{AB}, in a CCF the openings can be comparable, of the same order of magnitude. In addition to the ventilation holes, which can be easily measured and accounted for one or the other skin, there are other concentrated and distributed sources of permeability, strongly dependent on the design strategies, like for instance the structural silicone wet or dry gasket system to support the glass. Permeability exists indeed between gasket and glazing and its equivalent opening area changes depending on direction (pressure or suction) and magnitude of the net pressure, as the gap can be closed in one direction of pressure and open in the other one and it can be in general increasing when the net pressure increases. Or, quite often, it can have sudden transition from a quite constant equivalent opening area by the net pressure to a state of abrupt increase of permeability. In addition, other sources of permeability can occur because of unintended manufacturing variations, like unsealed mullion to transom connections and other gaps like screw holes. The level of designed permeability of the cavity is so low than any unexpected difference can have a non-negligible impact. For this reason, the authors believe that a custom design approach would be the most suitable response to the current uncertainties of the standards about the load sharing in double skins. For this purpose, the recent publications of [CWCT] pushes in the same direction. The manuals show exactly the same design guidelines published firstly in EN1991-1-4, but they state that it is possible to use different pressures than reported in the tables by detailed calculations or measurements based on actual façade construction. Also, they highlight that construction tolerances should be taken into consideration. Indeed, it should not be forgotten that sustainability is an important objective for the façade design, even considering safety always comes first. Furthermore, especially in the market of bespoke curtain wall it is often difficult to adopt simple rules of general application. The best compromise for an optimization stays a flexible calculation approach that accepts as input a series of façade geometries, materials and other characteristic inputs. With respect to the CCF, it will be evident that the permeability functions are the major unknown, while all the other façade parameters can be derived by well-established tools or calculated by validated algorithms. For this reason, the authors believe that a calculation assessment tool should be validated and used in conjunction with permeability functions derived by experimental testing when a new custom design without any reference is going to be used. Or, sensitivity analysis can be conducted, based on already existing data, previous experience and known scatter. It would be possible to improve the current code with a conservative approach by providing analytical approaches with general validity, but hence not fully optimized given the lack of specific input.

In the following document, the authors will report experimental results obtained for a sample unit of mfree-S^{CCF} manufactured for a recent project in London. The permeability functions discussed will be fundamental for the setup of the calculation approach that will be shown in the third paper, aiming to validate the proposed assessment tool in comparison with measurements of façade cavity pressure and displacements under superimposition of thermal loading, wind loading and air dry flow. In a first part the calibration test, part of the quality control procedure, will be discussed, giving the insights for the understanding of permeability levels and scatter among the different specimens. Then, in a second part, by means of static equalization pressure tests, a method to define the permeability function of a specific unit will be discussed.

Although presented in relation to the CCF façade type, the approach at hand is applicable to any type of compact double skin, for which the internal of the cavity could be reasonably considered as a confined volume in communication with established external or internal known pressures by means of surface openings. In particular, the benefit of a comprehensive assessment tool is clear because it can identify the range of permeabilities for which a certain effect is relevant. For this purpose, it will be seen that a CCF, in contrast to a ventilated double skin, introduces a significant impact of the air cavity temperature on the structural performance, as the reduced permeability does not allow a sufficient release of mass in time to avoid a consequent raise of pressure. However, it will also be concluded that the effect is not as relevant as assessed by a simple insulating unit equivalent scheme, which in this sense is an overly conservative calculation method, to be avoided in favour if a sustainable design.

2.Calibration tests

The CCF requires an accurate quality control protocol to maintain the high performance requirements during its entire service life. In particular, the value of permeability is a fundamental parameter that is critical for the performance adequacy. Like for the mfree-S^{CCF} facade project in object, with a geometry shown at the left side of Fig.2, each manufactured unitized façade panel is subjected to a calibration procedure, which should ensure that the permeability of the cavity will be maintained in a suitable range for the entire life of the façade. In literature a specific parameter, called air tightness K has been defined in order to characterize the permeability of the specimen:

$$K = \frac{Q}{P^{0.66}} \tag{1}$$

During the calibration test, represented in Fig.2 at the right side, a constant high flow Q_{HIGH} is applied to the panel, with a consequent buildup of the pressure from P_0 to P_1 in a certain time. After the first phase, a second phase starts with a Q_{LOW} application: after this phase the final pressure P_2 should remain in a certain range in order to accept the panel tightness as it is. Again a third phase with high flow will bring the pressure to the value P_3 and finally the P_4 pressure will be reached under a second period of low flow Q_{LOW}. Again the panel will be accepted only if P_4 will remain in the expected range of pressures. The overall duration of the test is a compromise between the expected confidence about the air tightness check and a request for a non-excessive increase of production time per unit. Even if variable in relation to the size of the unit, in general it takes around 10 minutes.

A set of calibration tests from the specific project is presented and analyzed below.

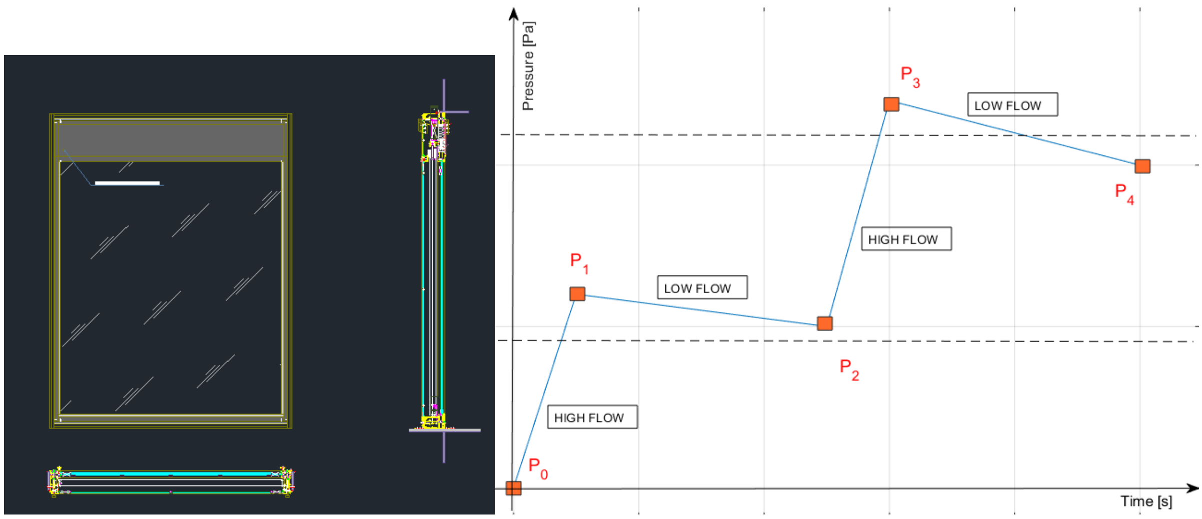

Fig. 2 Geometry of the unitized mfree-S^{CCF} panel analyzed (left) and schematic representation of the calibration procedure for a CCF panel

The set of calibration tests consists of more than one thousands runs on a different types of specimens and with different calibration procedure flows, as the flows have to be chosen on the basis of the panel geometry. 102 calibration tests have been selected, because they are characterized by exactly the same calibration test conditions and provide a representative statistical sample. Fig. 3 shows the 4 rates of pressure increase during the 4 phases previously described, with G_i the rate of the pressure increase or decrease in the corresponding phase of testing duration:

$$G_i = \frac{(P_i - P_{i-1})}{(t_i - t_{i-1})} \tag{2}$$

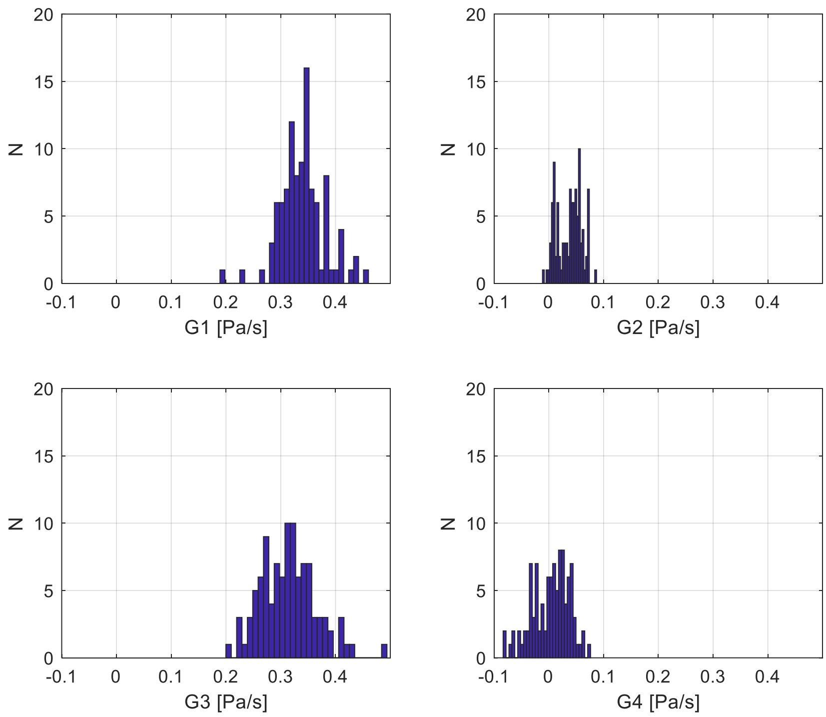

Fig. 3 Histograms of the 4 slopes G_1, G_2, G_3 and G_4 under the calibration tests for 102 specimens

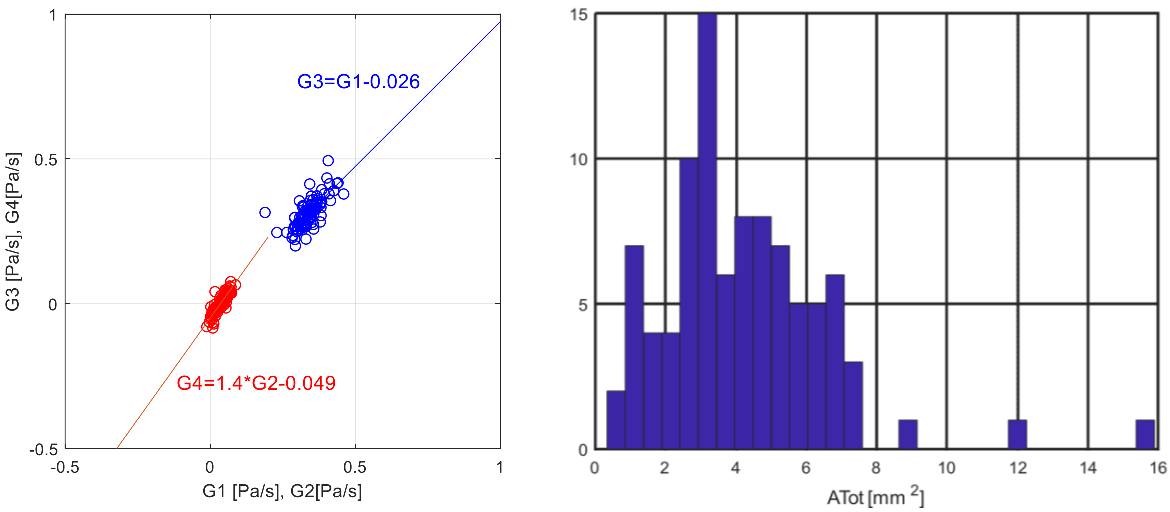

Fig. 4 Correlation between G1 and G3 and G2 and G4 slope of the test (left side) and histogram for 102 panels of back-calculated permeability by the tool

Fig. 4 at the left side shows the correlation between G1 and G3, from which it appears that G3 is in general smaller than the G1 for the same calibration test. In the same way, correlation between G2 and G4 shows that G4 is in average larger than G2. By means of the back calculation with the proposed numerical tool, searching for the total cavity permeability A_{TOT} that provides the best fitting of the numerical pressure time history with the measured one, the correlation between the permeability A_{TOT}, sum of the two permeability A_{RS} and A_{AB} and G_1 can be estimated. Fig. 4 (right side) shows the histogram of the probability density function for the back-calculated A_{TOT} of each specimen, while Fig. 5 shows the cumulative distribution functions of the back calculated permeability A_{tot}. It can easily be deducted that in general the permeability slightly increases for increasing values of cavity pressure, as shown by the G1-G3 and G2-G4 correlation.

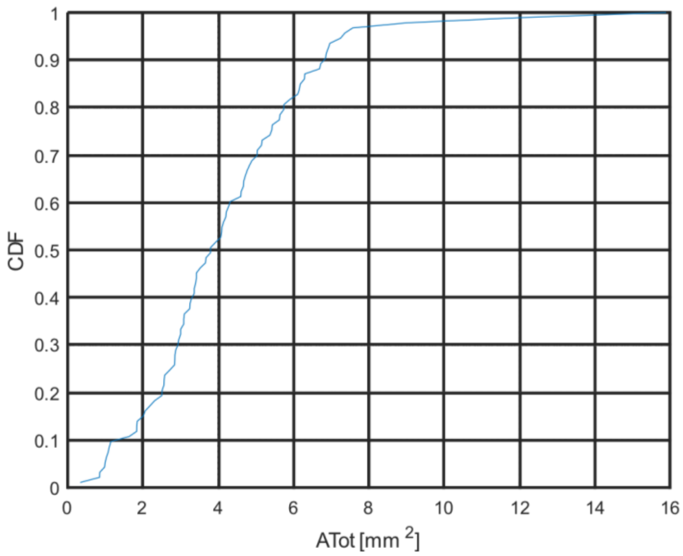

Fig. 5 Cumulative distribution function of the back-calculated A_{TOT}

Another confirmation occurs once the numerical tool is used to back-calculate the response of the cavity with the complete flow time history as input. As it can be seen in Fig. 6, when a constant permeability for the cavity is adopted, the fit is good during the first 2 phases of calibration, while the pressure is overestimated during phase 3 and 4 (green curve). On the contrary, when the permeability Atot is given as input as a function of the cavity pressure, with larger values at larger pressures, the blue curve is obtained.

The results of table 1 show how the estimated pressure is also highly sensitive to the composite action assumed for the laminated glass through the shear relaxation module of the PVB. Indeed, a larger or smaller Young Modulus would mean a different displacement of the laminated glass under the same cavity pressure, which in turn would mean a different volume variation of the cavity and then a different pressure at the equilibrium. In particular, a high composite action gives a small volume variation of the cavity under the elemental air flow, then a large increment of pressure occurs.

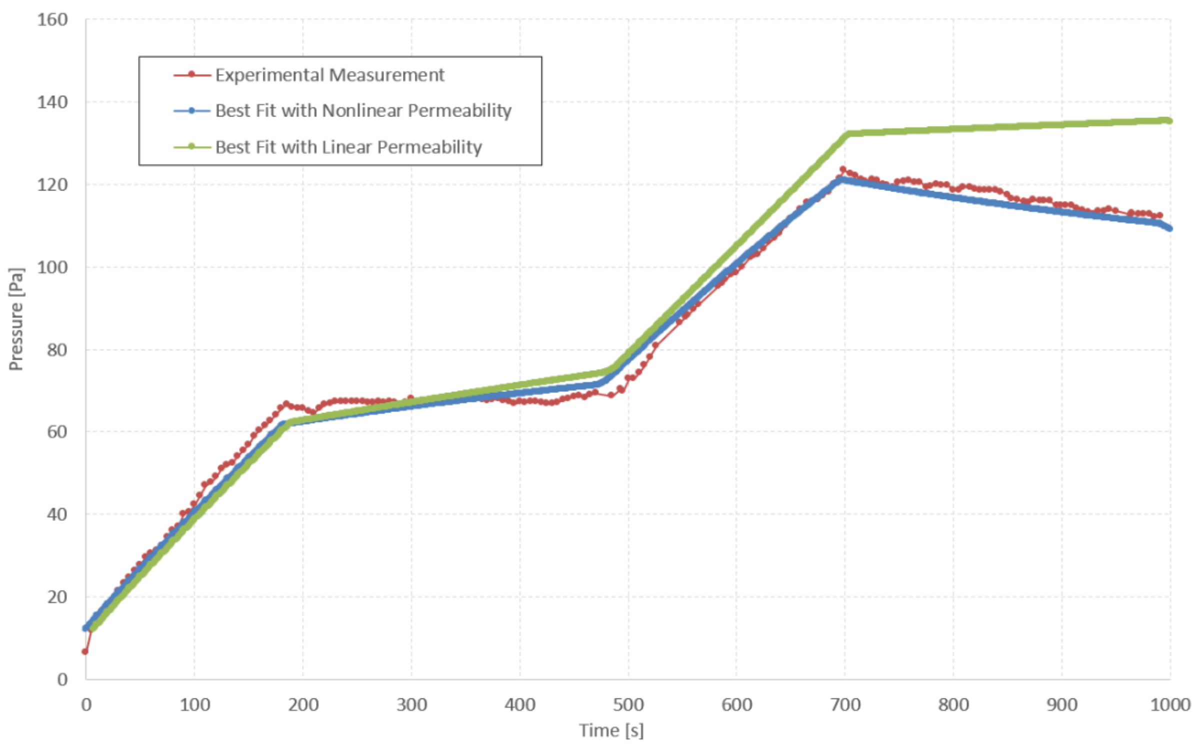

Fig. 6 Comparison between the cavity pressure measured during a calibration test on a façade specimen and the corresponding numerical best fitting with linear (constant) and variable non linear permeability function

On the contrary a small composite action gives a large volume variation and then a smaller pressure increase for the same flow. Table 1 is clearly showing this effect. For this reason, the calibration of the tool should consider relevant variation of load duration and temperature, in order to experience several relevant working conditions for the interlayer Young Module. Under the calibration test conditions, it seems that a Young Modulus 30000MPa for the PVB is most accurate. Indeed, making use of this value the average values of G1, G2, G3 and G4 as per Fig. 6 occur for the expected average values of the cavity permeability.

Table 1: G1, G2, G3 and G4 calculated by the numerical tool in function of the PVB Young Module and total cavity permeability

G1 rate [Pa/s]		Young Module [MPa]							
		0.3	1	10	100	1000	10000	30000	70000
Total Cavity Permeability [mm2]	0	0.109	0.1451	0.2198	0.2524	0.2672	0.3186	0.3992	0.5008
	1	0.1064	0.1411	0.2126	0.2435	0.2575	0.3061	0.3817	0.4763
	2	0.1038	0.1373	0.2055	0.2349	0.2482	0.294	0.3649	0.4528
	3	0.1012	0.1335	0.1987	0.2266	0.2391	0.2823	0.3487	0.4303
	4	0.0987	0.1298	0.192	0.2184	0.2303	0.271	0.3331	0.4087
	5	0.0963	0.1262	0.1856	0.2106	0.2218	0.2601	0.318	0.388
	10	0.0849	0.1095	0.156	0.1748	0.1831	0.2108	0.2512	0.2974
	20	0.0659	0.0818	0.1088	0.1186	0.1228	0.136	0.1532	0.1702

G2 rate [Pa/s]		Young Module [MPa]							
		0.3	1	10	100	1000	10000	30000	70000
Total Cavity Permeability [mm2]	0	0.0441	0.0556	0.0807	0.0921	0.0972	0.1151	0.1434	0.1803
	1	0.0385	0.0478	0.0672	0.0756	0.0794	0.0923	0.1118	0.136
	2	0.0333	0.0406	0.0548	0.0606	0.0632	0.0716	0.0835	0.0969
	3	0.0286	0.0338	0.0434	0.0469	0.0484	0.0529	0.0583	0.0626
	4	0.0241	0.0276	0.0329	0.0345	0.035	0.0361	0.0358	0.0325
	5	0.0199	0.0219	0.0235	0.0232	0.0228	0.0209	0.0158	0.0062
	10	0.0035	-0.0007	-0.0127	-0.0189	-0.022	-0.0331	-0.0519	-0.0771
	20	-0.0148	-0.0238	-0.0423	-0.0496	-0.053	-0.0629	-0.0759	-0.0884

G3 rate [Pa/s]		Young Module [MPa]							
		0.3	1	10	100	1000	10000	30000	70000
Total Cavity Permeability [mm2]	0	0.1636	0.1978	0.2765	0.3133	0.33	0.3876	0.4804	0.6072
	1	0.1503	0.1808	0.249	0.2805	0.2946	0.3431	0.4197	0.5213
	2	0.1385	0.1655	0.225	0.2521	0.2642	0.3053	0.3691	0.4515
	3	0.1278	0.152	0.2042	0.2275	0.238	0.2732	0.327	0.3947
	4	0.1181	0.1399	0.186	0.2064	0.2155	0.246	0.2919	0.3486
	5	0.1095	0.1291	0.1703	0.1882	0.1962	0.2229	0.2627	0.3111
	10	0.0777	0.0907	0.1176	0.129	0.134	0.1509	0.1764	0.2071
	20	0.0481	0.0578	0.0775	0.0854	0.0888	0.0998	0.1143	0.128

G4 rate [Pa/s]		Young Module [MPa]							
		0.3	1	10	100	1000	10000	30000	70000
Total Cavity Permeability [mm2]	0	0.0688	0.0811	0.1111	0.1254	0.1318	0.1545	0.1915	0.2434
	1	0.0531	0.0607	0.0787	0.0866	0.0901	0.1017	0.1194	0.1418
	2	0.0397	0.0437	0.0521	0.0553	0.0566	0.0603	0.0644	0.0672
	3	0.0284	0.0295	0.0306	0.0302	0.0298	0.0278	0.0225	0.0123
	4	0.0189	0.0177	0.013	0.0099	0.0084	0.0022	-0.0097	0.0285
	5	0.0108	0.0077	-0.0013	-0.0063	-0.0087	- 0.018	-0.0346	-0.0588
	10	-0.0136	-0.0218	-0.0414	-0.0506	-0.0549	-0.07	-0.0938	-0.1234
	20	-0.0271	-0.0366	-0.0552	-0.0622	-0.052	-0.0747	-0.0866	-0.0975

3.Quasi-static tests. Permeability functions

An efficient assessment tool for the estimation of the double skin façade behaviour under wind loading should properly account for both the skin stiffness interaction with the cavity and the permeability towards the different boundary conditions, generally external and internal building pressures. While the stiffness contribution of the skins and the behaviour of the gas in the cavity can be derived in a straightforward way by means of the analytical formulations, the skin permeability components A_{RS} and A_{AB} are critical elements for the assessment of the cavity pressure in a CCF, probably more so compared to other types of double skin facades. The reasons have been discussed in the previous paragraph and can be summarized in two major items:

- The Scatter of the permeability is not negligible and must be taken into account in the pressure assessment for design purposes

- The Permeability of the almost impermeable CCF skin is characterized by a “nonlinear” behaviour as a function of the net pressure applied

The two items are actually typical for every double skin façade, but in the specific case of the closed cavity the topic relevance is of upmost importance, because of the small level of permeability involved and because of the similar values of permeability that can be accounted for rain screen side and air barrier side of the same skin, leading to larger uncertainties/variations in the load sharing behaviour itself.

In general, permeability is composed of intended surfaces of flow (like slots and holes for ventilation) and unintended leaks, concentrated in specific locations (like framing connections, unsealed screws) or distributed along edges, like in case of the interface between glazing and supporting frame, where the glass is mechanically fixed. An ideal procedure should start from the knowledge of the cavity permeability functions, in terms of its skin permeability components, still expressed according to the classical rainscreen and airbarrier representation $A^{+}_{AB}(P)$, $A^{-}_{AB}(P)$, $A^{+}_{RS}(P)$, $A^{-}_{RS}(P)$, where the notation “+” and “-“accounts for the fact that the permeability is not necessarily symmetric with respect to the pressure direction. Then in general 4 functions should be known for each cavity, assuming that it is in communication with two pressure environments, while additional terms appear when communication with other cavities exists (mutual permeability). However, it is questionable whether an approach based on the assembly of the single permeability function in isolation would be consistent with the actual behaviour of the manufactured panel. Indeed, permeability of the skin is strongly dependent on interactions between framing supports and closure surfaces and probably the best approach consists of the evaluation of the skin permeability under actual working conditions. On the other hand, as it will be shown in paragraph 3.1, an experimental layout cannot directly give the permeability skin functions in a single run, but they must be determined from a series of their combinations by means of appropriate back-calculation and best fit of the experimental results.

3.1.Experimental lay-out

A panel with the same construction details of the unit shown in section 2 has been subjected to a sequence of static pressure tests according to the list shown in Table 2. Two positions have been adopted for the panel as shown in Fig. 7: position 1, with the actual inner skin double glazing unit facing the pressure box and the other one (position 2), simulating the real working conditions, with the (outer) single laminated glass facing the pressure box. Two different manufacturing scenarios, simulating sealing mistakes and multiple opening/closure of the cavity have been also considered. Scenario 2 in particular has been obtained by sealing a gap in a screw at the spandrel area, which was on the contrary open into the Scenario 1.

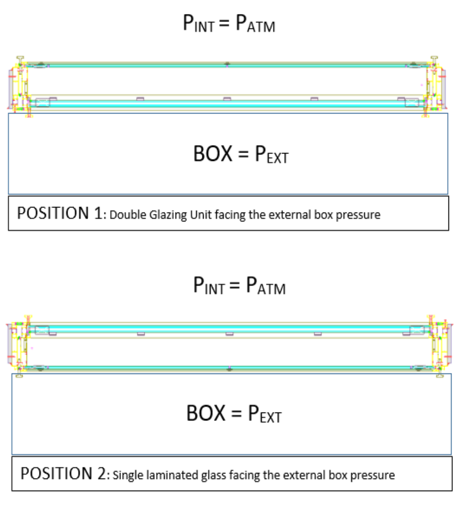

Fig. 7 Position 1 and Position 2 of the façade unit with respect to the testing box pressure

Table 2: Quasi Static Test Summary (CAL stays for Cavity Air Leakage)

Test Number	Type	Flow	Scenario and Position
1	Static Pressure	NO	Scenario 1 / Position 1
2	Static Suction	NO	Scenario 1 / Position 1
3	Pulse Suction	NO	Scenario 1 / Position 1
4	CAL Pressure	NO	Scenario 1 / Position 1
5	Static Pressure	YES (100l/h)	Scenario 1 / Position 1
6	Static Suction	YES (100l/h)	Scenario 1 / Position 1
7	Pulse Suction	YES (100l/h)	Scenario 1 / Position 1
8	Calibration Test	-	Scenario 1 / Position 1
9	Water-Tightness	-	Scenario 1 / Position 1
10	Calibration Test	-	Scenario 1 / Position 1
11	Calibration Test	-	Scenario 1 / Position 2
12	CAL Pressure	NO	Scenario 1 / Position 2
13	Static Pressure	NO	Scenario 1 / Position 2
14	Static Suction	NO	Scenario 1 / Position 2
15	Pulse Suction	NO	Scenario 1 / Position 2
16	Static Pressure	YES (100l/h)	Scenario 1 / Position 2
17	Static Suction	YES (100l/h)	Scenario 1 / Position 2
18	Pulse Suction	YES (100l/h)	Scenario 1 / Position 2
19	Calibration Test	-	Scenario 1 / Position 2
20	Calibration Test	-	Scenario 2 / Position 2
21	CAL Pressure	NO	Scenario 2 / Position 2
22	Static Pressure	NO	Scenario 2 / Position 2
23	Static Suction	NO	Scenario 2 / Position 2
24	Pulse Suction	NO	Scenario 2 / Position 2
25	Calibration Test	-	Scenario 2 / Position 2

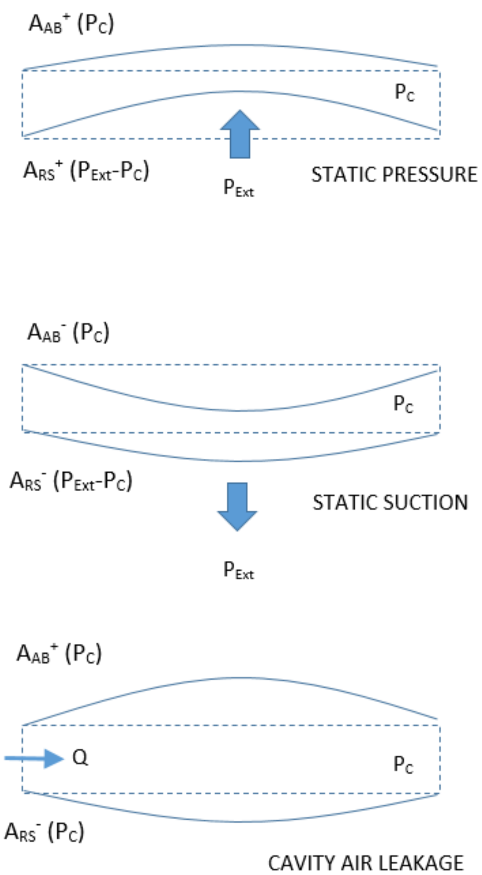

Fig. 8 Skin permeability components

As shown in Fig. 8, the different static tests (pressure, suction and cavity ar leakage) supply relations between the different components of the skin permeability, but in general it is not possible to derive the permeability in pre-determined pressures as solution of a system of linear equations: as it will be shown in paragraph 3.3, a best fit approach based on least square method for instance can be used to assess coefficients of polynomial functions to fit the experimental relations.

3.2.Results

Out of the obtained results, in this section the most relevant conclusions in terms of impact of the permeability on the pressures at the equilibrium will be shown. It must be noted like test 20 and following have been performed on a façade system that should be different from the previous one tested, being subjected to several modifications with potential impact on the air tightness. Indeed, after test 19, the external laminated glass has been removed and thermocouples have been installed on the panel in order to prepare it for the subsequent experiment into the climatic testbox (scenario 2). In addition, a screw that was left unsealed into the scenario 1 has been sealed, in order to simulate different manufacturing result.

Fig. 9 shows the comparison of the pressure at the equilibrium during test 12 and 21. Considering the system of two equations for the equilibrium of the double skin cavity and the DGU cavity and being null all the mutual permeability terms (fully closed DGU cavity), we can write for the double skin cavity with index 1 (index 2 is assigned to the double glazing unit cavity):

$$Q_1 + A_{1RS-eq}\sqrt{\frac{2(P_{c1})}{\rho}} + A_{1AB-eq}\sqrt{\frac{2(P_{c1})}{\rho}} = 0 \tag{3}$$

Where the “eq” subscript means that the coefficient takes already in account also the related discharge coefficient. From (3) it is easy to derive that:

$$A_{1TOT-eq} = A^{-}_{1RS-eq} + A^{+}_{1AB-eq} = \frac{Q_1}{\sqrt{\frac{2(P_{c1})}{\rho}}} \tag{4}$$

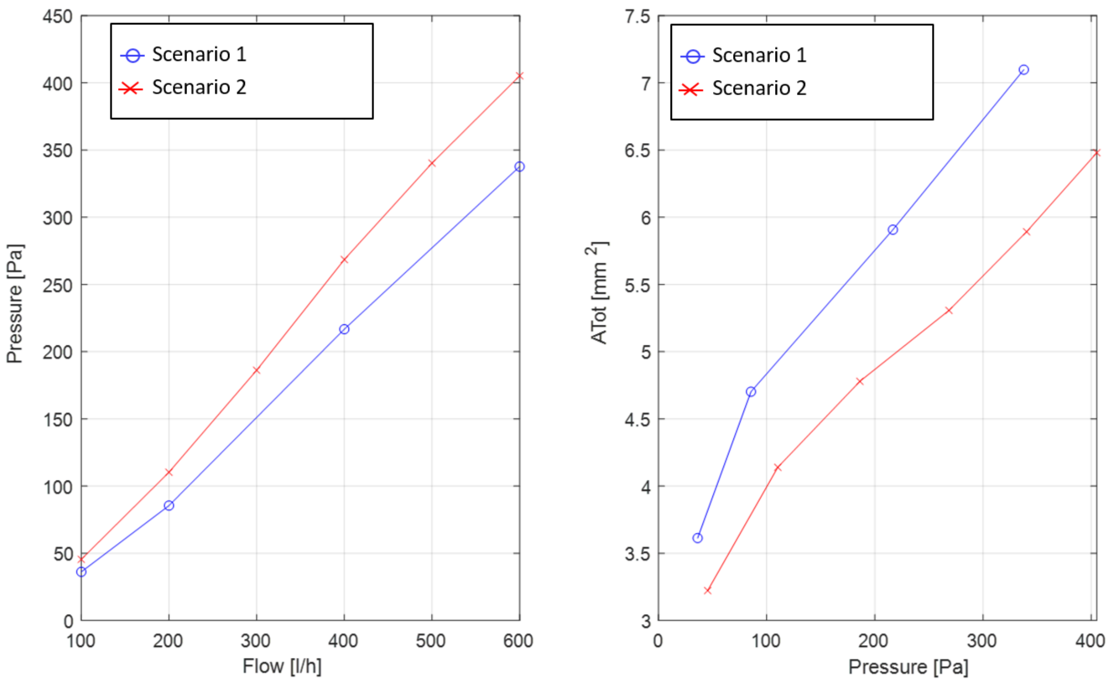

Fig. 9 Pressure build up and equivalent cavity permeability under different flow rates

It can be seen that the air tightness is increased after the thermocouples installation, regardless of the new holes provided for the wires. On the contrary, it has been for sure important to seal the screw hole, as the permeability appears to be reduced by a 10-15% in the whole pressure range investigated. However, it must be reminded that the total permeability deducted by this test is the sum of the outer skin permeability in outward direction and inner skin in inward. Not necessarily the same directions will be reflected by the pressure or suction test, which on the contrary involves the combination of the permeability in the same direction, but not for the same pressure difference. Considering these statements and making use of Latta equation, the eq.(5) can be written.

$$\frac{P_C}{P_{Ext}} = \frac{1}{\left(1+\left(\frac{A_{AB}(P_C)}{A_{RS}(P_{Ext}-P_C)}\right)^2\right)} \tag{5}$$

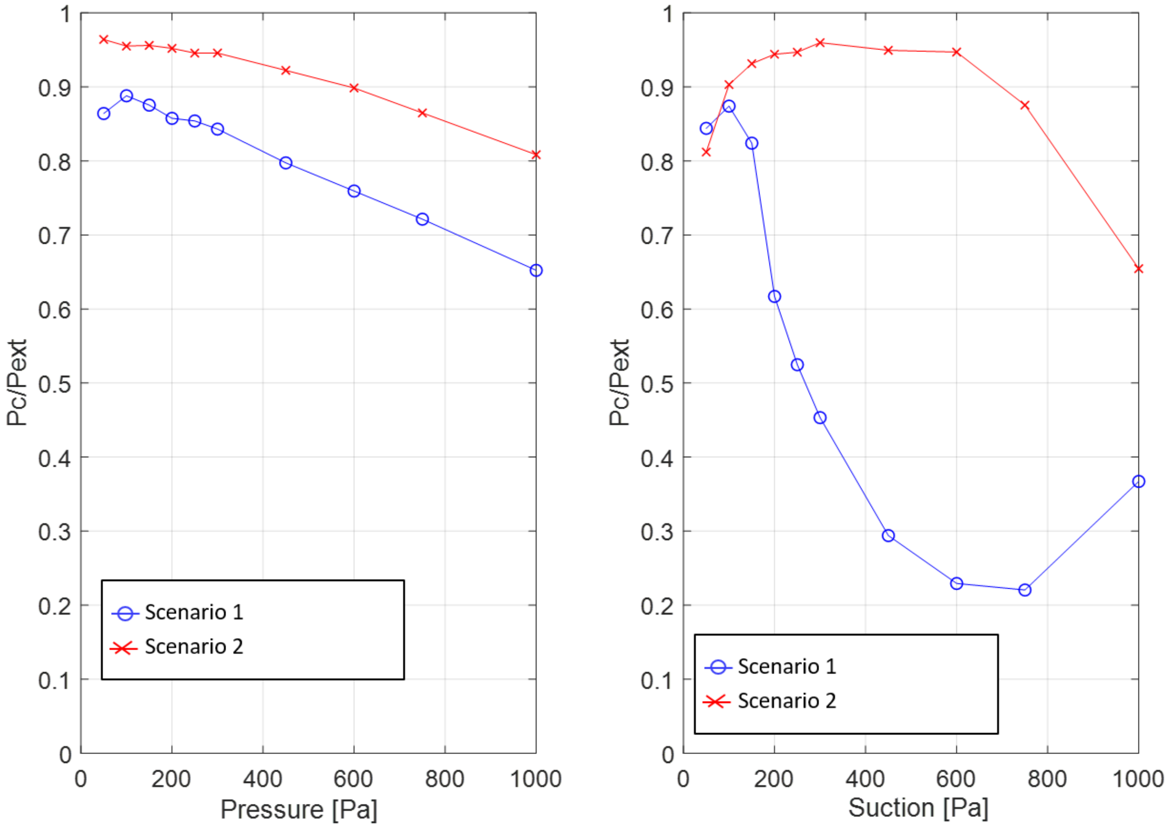

Fig. 10 Pressure in the cavity under different conditions of applied external pressure. The results are taken from Tests 1 (Static Pressure) and 2 (Static Suction) for Scenario 1 and Tests 22 (Static Pressure) and 23 (Static Suction) for Scenario 2

From the observation of Fig.10, on the contrary, we can assess the changes of the cavity pressure against pressure and suction wind load application. The results refer to the tests 1,2, 22 and 23 of Table 2. As the response of the cavity versus the induced dry air flow involves the total leakage (eq. (4)), the pressure and suction test gives information about the repartition of the leakage according to eq. (5). It appears that after the thermocouple installation the cavity is in general more pressure-equalized toward the external, then A_{RS} appears larger than A_{AB}. In case of the behavior against positive pressure, it could be concluded that because of the sealed hole at the inside skin, the A_{AB} contribution is reduced, resulting in a larger ratio P_c/P_{Ext}. On the contrary that effect is not relevant under suction (the screw head under suction was anyway closing the gap), indeed it is not visible a difference under suction behavior at the small negative pressure levels. However, above the 100Pa the ratio P_c/P_{Ext} after the thermocouple installation increases and remains stable, while in the range 100/800Pa, prior to the thermocouple installation the suction in the cavity at the equilibrium was significantly smaller. For sure this is due to another effect, probably related to a better tightness of the air barrier (inner skin) under suction: this evidence highlights that significant difference in the pressure ratio and then in the air leakage ratio can appear at the large pressures. However, it must also be highlighted that in order to achieve the stability of the pressure, a single pressure step has required around 30minutes of differential pressure application due to the low air permeability: is this time duration relevant under wind load design?

3.3.Permeability function estimation

As discussed, the knowledge of the permeability versus net pressure for the single skins (in inward and outward directions) are required in order to simulate the cavity pressure at the equilibrium under different loading actions. However, the experimental test sequence investigated in this paragraph and shown in table 2 does not directly give the functions, but only combinations of their values at different pressure values.

In order to estimate the $A^{+}_{AB}(P)$, $A^{-}_{AB}(P)$, $A^{+}_{RS}(P)$, $A^{-}_{RS}(P)$ in an accurate way, the following approach is proposed. At least the following tests should be performed in order to run an assessment procedure:

- A cavity air leakage test under cavity positive pressure by an air dry flow, without applied external pressure.
- A pressure static test at different steps of pressure applied on the external skin of the facade
- A suction static test at different steps of pressure applied on the external skin of the facade
- A cavity air leakage test under suction or in alternative a pressure/suction test with the application of a constant flow

Due to technical limitations, it has not been possible to perform the cavity air leakage test under suction, for this reason the best fit makes use of a sequence of tests under dry air flow application in conjunction with those ones without flow.

1) Analytical model selection for the positive and negative pressure permeability functions A_{AB}^{+} and A_{AB}^{-}, for instance, polynomial of second order. Higher polynomial orders can be used, with a higher impact on the calculation effort.
2) Hypothesis of relatively constant leakage for a small pressure range (likewise linear behavior) [0,PLin]. For typical applications this value can be chosen as 50Pa. This value can be considered in first approximation independent on net pressure direction.
3) Eq. (5) and Eq. (4) are used in order to derive the working points for the A_{RS}^{+} and A_{RS}^{-}. A substitution in Eq. (5) is done making use of the results of the test with dry air flow
4) Best fit by means of least square approximation is conducted in order to derive the polynomial form of A_{RS}^{+} and A_{RS}^{-}
5) The combination of the polynomial A_{AB}^{+}, A_{AB}^{-}, A_{RS}^{+} and A_{RS}^{-} of minimal difference with the experimental cavity pressures under the static pressure and suction test with flow is calculated, looking for the optimal polynomial coefficient series by the least square approximation method.

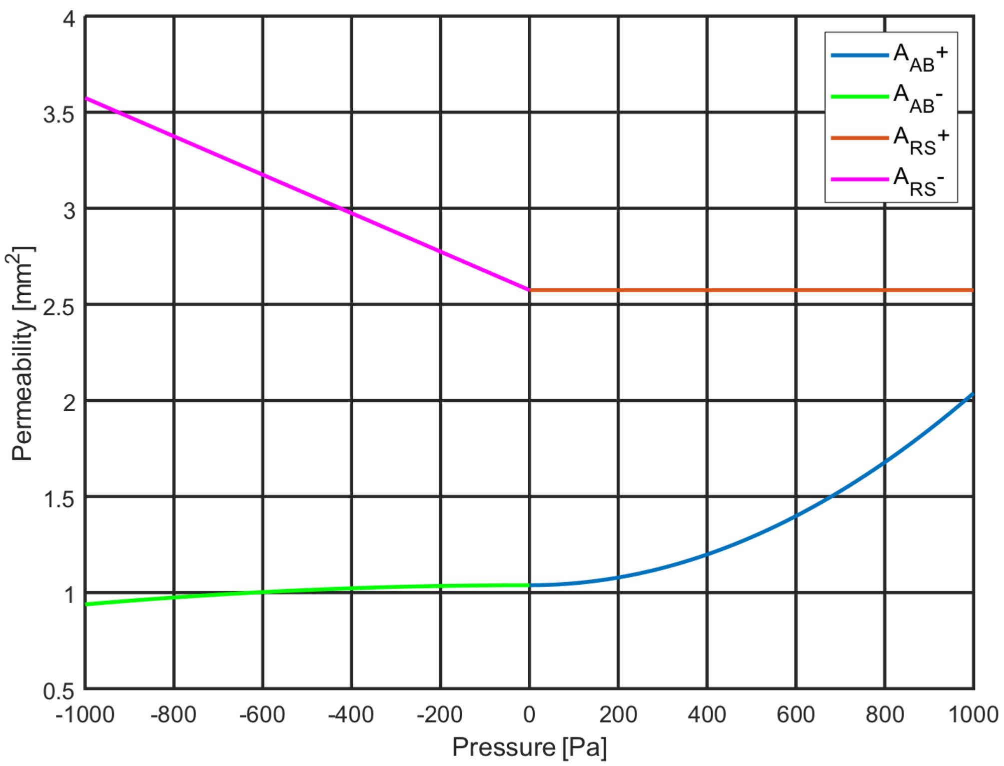

Fig. 11 Best fit for the permeability functions using test data 12, 13 and 14 according to the described optimization procedure

In Fig.11 the result of the procedure applied by the test data test 12, test 13 and test 14 of Table 2 is shown in terms of permeability functions of the skins against the net pressure, both in inward and outward directions. It can be seen that the rainscreen tightness (outer skin) is quite constant for positive (inward) net pressures, while it increases significantly for negative (outward) net suction. On the contrary the airbarrier (inner skin) permeability increases under net positive pressures and it remains quite constant under net suction. Another interesting observation is that the airbarrier shows a quite stable slope crossing the zero pressure, while the slope of the rainscreen permeability has an abrupt change, which is probably the effect of a concentrated leakage that impact the tightness only in outward direction. On the contrary, constant slopes across the zero, but with a continuous increasing rate of permeability versus pressure reflects the behavior of the glazing support versus the pressure application. In this sense, the strategy adopted whether dry glazed or structurally silicone and the geometry of the support solution will have the major impact in the nonlinear trend of the permeability functions. Experimental testing, coupled with an optimization approach to back calculate polynomial functions, or numerical assessment by fluid structure interaction analysis seem the only viable methods to retrieve the permeability functions and to apply a complete assessment for the estimation of the cavity pressure under wind and temperature loading.

As it has been shown in chapter 2, any possible manufacturing mistake can significantly change the load sharing between the outer and inner skin, reason why a dedicated quality control should be conducted in order to support a calculation strategy based on the methodology shown in this chapter. Indeed, the practical application of the methodology should rely on the acquisition of results on static and cavity air leakage testing on one or few samples, assuming a scatter of the permeability of external and internal skin that should not exceed reasonable values among the different manufactured façade units.

4.Conclusions and future work

This paper is the second work of the authors within a full scope of three documents, aiming to highlight the need for an accurate assessment tool for the double skin structural behavior calculation, with particular attention to the novel CCF façade typology. By means of the first paper, a discussion about the theoretical findings and a proposed algorithm for the load sharing-pressure equalization has been held. In this specific paper, the objective has been the characterization of the permeability behavior of a CCF, describing in detail the level of the scatter of its openings due to the manufacturing and calibration process and the particular nonlinear behavior against the net pressure. An analytical empirical approach based on experimental measurements has been presented for the evaluation of the skin permeability functions to give as input to the assessment tool. In the third and final paper, the authors will show how the assessment tool gives estimations in line with the outdoor displacement and pressure measurements on a specimen subjected to the climatic and wind loading variations. Finally, a comparison between simulations carried out by the assessment tool and through standard calculation approaches will be conducted, showing the evidence that an opportunity for an improvement of structural calculation methods for double skin exist, towards the target of a more sustainable façade design.

5.References

[1] EN 1991-1-4. Eurocode 1: actions on structures – Part 1-4: general actions – wind actions. CEN, Brussels, Belgium; 2005.
[2] Guidance on built up walls, CWCT, 2017
[3] Guidance on the actions of non-load bearing building envelopes, CWCT, 2017
[4] Laverge J., Schouwenaars S., Steeman M., Janssens A., Van Den Bossche N., Condensation in a closed cavity double skin facade: a model for risk assessment. Building Envelope Systems and Technologies (2010): 125-134, Vancouver.
[5] Van Den Bossche N., Janssens A., Moore T., Lacasse M., Development of a numerical model for pressure equalization in facades during wet conditions. Building and Environment 178 (106919), 2020.
[6] Theory Manual Version 5.0. October 2018. Mepla software for structural glass design.
[7] Ghaffarian Hoseini, Ali, Ghaffarian Hoseini, Amirhosein, Berardi, U., Tookey, J., Li, D.H.W., Kariminia, S., 2016. Exploring the advantages and challenges of doubleskin facądes (DSFs). Renew. Sustain. Energy Rev. 60, 1052–1065. https://doi.org/10.1016/j.rser.2016.01.130.
[8] Poizaris, H., 2004. Double skin facades for office buildings: literature review. Tech. Rep. , Report EBD.
[9] Gerhardt, H., Kruger, O., 1997. Double skin glass facades-investigations into the load sharing possibilities. In: Proc. Of ICBEST, vol 97, pp. 335–339.
[10] Van Den Bossche, Nathan, Arnold Janssens, Michael Lacasse, and Travis Moore. 2013. "The Impact of Pressure Equalization on Watertightness of Rainscreen Systems." In Contributions to Building Physics, ed. A Mahdavi and B Martens, 783–790.
Wellershoff F., Bemessungsschubmodulwerte für Verbundglasscheiben, **https://doi.org/10.1002/stab.200710021**
[11] Van Den Bossche N., Watertightness of building components: Principles, Testing and Design Guidelines. Ghent University, 2013
[12] Burgess, J.C., McCardle, G.,, Building cladding air pressure equalization investigations – comparison between field results and numerical model, Building and Environment 35 (2000) 251-256

[13] Baskaran, B.A., Review of Design Guidelines for Pressure Equalized Rainscreen Walls, National Research Council Archive
[14] Ganguli , U., Dalgliesh., W.A., Wind pressures on open air screen walls: Place Air Canada, Journal of Structural Engineering 114, 3 March 1968, 642-656
[15] Straube, J., Pressure moderation and rain penetration control, " Proceedings of the Ontario Building Envelope Council (OBEC) Pressure-Equalized Rainscreen (PER) Seminar 2001, University of Waterloo, Waterloo, Ontario, 2001, pp. 1-51.
[16] Ganguli U., Quirouette R.L,, Pressure equalization performance of a metal and glass curtain wall, Proceedings CSCE Centennial Conference, Montreal 1987, Vol.1, 127-144
[17] Straube, J., Moisture control and nclosure wall system, PhD thesis, Civil Engineering Department, University of Waterloo, April 1998
[18] Ishida, H., Double skin glass façade-Design Method of wind pressure, Glass Processing Days 2003
[19] Baskaran, A., A numerical model to elevate the performance of pressure equalized rainscreen walls. Building Environment 1994